Co-published by
Institute of Fluid-Flow Machinery
Polish Academy of Sciences
Committee on Thermodynamics and Combustion
Polish Academy of Sciences

http://www.imp.gda.pl/archives-of-thermodynamics/

Impact of thermal modernisation including heat source replacement on the heating load of an existing single-family building in Poland

Wiktoria Bernat, Katarzyna Zwarycz–Makles*

Department of Heating, Ventilation and Heat Engineering, Faculty of Civil and Environmental Engineering,
West Pomeranian University of Technology in Szczecin, al. Piastow 17, 70-310 Szczecin, Poland
*Corresponding author email: kzwarycz@zut.edu.pl

Received: 20.10.2025; revised: 24.11.2025; accepted: 25.11.2025

Abstract

This study presents a comprehensive analysis of the impact of thermal retrofit, including the heat source modernisation, on the heating load of an existing single-family building located in Szczecin, Poland (Climate Zone I). The building, constructed in 2002, originally lacked thermal insulation in the walls, roof and ceiling, resulting in high operating costs and difficulties in maintaining thermal comfort. The aim of the project was to reduce heat losses, improve energy efficiency and enhance user comfort. The scope of work included thermal insulation of external walls, roof insulation, insulation of the intermediate floor slab and exterior wall section adjacent to the door opening and to the fenestration opening. The analysis conducted using the Audytor OZC 7.0 Edu Pol software showed that the total heat load of the building decreased from 25 710 W to 9476 W, representing a reduction of over 63%. Special attention was given to the analysis of thermal bridges, which are significant sources of energy loss. Using Therm 7.8.77 software, solutions were designed to reduce heat losses in critical areas. The heat transfer coefficients (*U*-values) for these thermal bridges were significantly reduced – by more than 50% in some cases. As part of the heat source modernisation, the solid fuel boiler and liquefied gas tank were removed and replaced with a condensing gas boiler powered by natural gas from the municipal network. To support the domestic hot water preparation system, flat-plate solar collectors were designed to work in conjunction with the existing dual-coil storage water heater.

Keywords: Thermal retrofit; Thermal modernisation; Heat source modernisation; Heating load; Thermal bridges

Vol. 46(2025), No. 4, 75–87; doi: 10.24425/ather.2025.156838

Cite this manuscript as: Bernat, W., & Zwarycz–Makles, K. (2025). Impact of thermal modernisation including heat source replacement on the heating load of an existing single-family building in Poland. *Archives of Thermodynamics*, 46(4), 75−87.

1. Introduction

Thermal retrofitting of existing buildings is one of the key measures aimed at reducing energy consumption and improving the energy efficiency of the residential sector. The scope of thermal retrofit depends on the specific conditions and needs of a given building and typically includes thermal insulation of external walls, roofs, and slab-on-grade floors, replacement of windows and doors, implementation of renewable energy sources and modernisation of heating and domestic hot water systems. The use of appropriate thermal insulation materials enables achieving low values of the overall heat transfer coefficient of building envelope components [1].

According to the Polish Act of Law of November 21, 2008, on supporting thermal modernisation and renovations, as well as on the central register of building emissions (Journal of Laws 2024, item 1446, as amended [2]), thermal retrofitting projects aim to reduce the demand for energy supplied to buildings, limit primary energy losses in local heating networks and heat sources, lower energy acquisition costs through heat source mo-

Nomenclature

A – area, m^2
b – correction factor
c_p – specific heat, J/(kg·K)
e_k, e_l – correction factors for location
f – correction factor
G_w – correction factor for groundwater influence
l – length, m
t – temperature, °C
U – coefficient of heat transfer, W/(m^2·K)
$\dot{V}_i$ – volume flow rate, m^3/s

Greek symbols

θ – temperature, °C
ρ – density at temperature $\theta_{int,i}$, kg/m^3
ψ – linear thermal transmittance coefficient, W/(m·K)
Φ – heat loss/heat power, W
Φ_{HL} – heat load, W

Subscripts

e – external
equiv – equivalent
g – ground
inf – infiltration
int, *i* – internal
i, *j* – heated space
k – building element
l – thermal bridge
RH – reheating
T – transmission
u – unheated space
V – ventilation

Abbreviations and Acronyms

COP – coefficient of performance
DHW– domestic hot water
EPS – expanded polystyrene
PVC – polyvinyl chloride

dernisation or energy recovery and shift to renewable heat sources. Therefore, uninsulated buildings should undergo thermal retrofitting due to economic, environmental and social considerations. The main reasons include energy and cost savings during operation, reduction of CO_2 emissions generated during heat production for space heating and improvement of residential comfort [3].

A significant improvement in energy efficiency, as well as enhanced thermal comfort for occupants, was documented in the study by Krause [4]. Following a comprehensive thermal retrofit of a single-family house, including insulation of external walls, the basement and the flat roof, replacement of windows and doors, installation of a new boiler and the implementation of a fireplace system with heat distribution, the seasonal heat demand was reduced by 87%, reaching a level of 11 430 kWh/year.

In a next study focused on optimising the retrofit of a single-family house built in 2007 in Warsaw, the authors (Zawada and Rucińska [5]) reported a 23% reduction in primary energy consumption and a 50% decrease in the thermal discomfort index following the proposed thermal modernisation. These results demonstrate that insulating the walls and roof, along with replacing windows with units featuring lower heat thermal coefficients, improves the building's heat balance during winter and enhances user comfort in summer.

The authors of publication [6], which evaluates the effects of thermal retrofit of single-family buildings, note that replacing window joinery alone results in a 3% reduction in heating energy consumption. Insulating external walls and the roof enables a 26% decrease, while comprehensive thermal modernisation, including upgrading the heat source, sealing building partition components, and improving ventilation, can reduce energy consumption by up to 59%. These improvements lead to a tangible reduction in heating costs and enhanced thermal comfort for occupants.

In the book edited by Koczyk and Antoniewicz [7], it is indicated that thermal retrofitting measures involving the insulation of all building envelope components and the reduction of ventilation rates can lead to significant energy savings ranging from 34% to 50% in terms of building heat load and heat demand. These findings demonstrate that thermal retrofit efforts positively influence building usability and contribute to a reduction in operational costs.

Contemporary challenges in building energy efficiency increasingly draw designers' attention to the issue of thermal bridges, which remain a significant source of heat loss in buildings. According to the study by Kurtz and Gawin [8] on the energy certification of residential buildings, thermal bridges are defined and exemplified as areas within the external envelope structure where a reduction in the internal surface temperature and an increase in heat flux density (heat loss) are observed relative to the surrounding components. Thermal bridges are categorised as linear or point-type, and both can lead to water vapour condensation and mould growth inside the building.

Roof thermal bridges are a critical source of heat loss in buildings [9], typically located along roof edges and around structural elements. These areas contribute to localised drops in interior surface temperatures and increased energy demand to compensate for the losses. One method for detecting thermal bridges is thermographic measurement using drones, which enables the identification of even minor existing thermal bridges.

The significance of thermal bridges in the context of building thermal modernisation, particularly their impact on heat loss and indoor microclimate, is discussed in [10]. Thermal bridges are a major source of heat loss, substantially contributing to reductions in internal temperatures. Therefore, effective thermal retrofit should include not only insulation of building envelopes but also of structural joints of the building. Thermal bridges account for approximately 16% of heat loss through building partitions, corresponding to around 7.8 kWh/m² of annual heat loss. To mitigate these losses, insulation connections must be consciously designed, which leads to cost reductions and improved comfort in residential buildings [11].

The issue of improving the energy performance of buildings and meeting legal requirements in this area is discussed in the study by Żarski [12], where the author emphasises that a key condition for effective building modernisation is a comprehensive approach encompassing both the structure of the building envelope and technical installations. The study highlights the

importance of including thermal bridges in the building's heat balance, in accordance with the guidelines of the PN-EN ISO 14683 standard, as even with high levels of envelope insulation, linear losses can significantly affect energy performance indicators.

The inclusion of thermal bridges in the assessment of building energy efficiency is thoroughly addressed by Pawlak [13], who emphasises that thermal bridges represent one of the key sources of heat energy loss and should be mandatorily considered in calculations of a building's thermal performance. The author points out that neglecting their impact may lead to significant discrepancies between the theoretical energy balance and the actual heat demand.

Study [14] investigates user activity in residential buildings through surveys and interviews, highlighting its impact on thermal-flow processes and energy consumption. Six behavioural profiles were developed and implemented in hourly dynamic simulations using DesignBuilder software to assess heat demand and indoor microclimate in selected Norwegian cities. Internal heat gains from occupants, appliances and solar radiation accounted for 20–35% of the energy balance, confirming the need for precise behavioural modelling. The authors advocate for hourly calculation methods over simplified monthly approaches, especially in the context of climate change. Accurate input data and increased public awareness are essential for improving energy efficiency and retrofit planning.

In Poland, the use of renewable energy systems in building design has grown due to regulatory requirements limiting primary energy consumption. A hybrid system combining ground-source and air-source heat pumps powered by photovoltaic electricity was installed in a facility near Kraków to evaluate performance and optimise energy use [15]. Both heat pumps showed comparable efficiency during the heating season, with coefficient of performance (COP) values of 2.69 and 2.63, respectively, suggesting that air-source heat pumps may be a cost-effective alternative. However, summer operation revealed reduced efficiency due to standby energy consumption. Integration with photovoltaic systems significantly improved ecological and economic performance, with self-consumption rates exceeding national averages. The findings support the broader adoption of renewable energy sources in construction and highlight the importance of accurate system design and climate considerations.

This study presents the impact of thermal retrofit on the heat load of a single-family building located in Szczecin (Polish Climate Zone I), which, due to the lack of thermal insulation, generated high operating costs and was associated with difficulties in maintaining the interior spaces, as reported by the occupants. The analysis included the influence of thermal bridges on heat losses. Additionally, the previously non-habitable attic was converted into a heated and residential space. The heat source was modernised by removing the solid fuel boiler and propane tank and replacing them with a condensing gas boiler connected to the municipal natural gas network. The project was complemented by the installation of flat-plate solar collectors for the domestic hot water (DHW) system.

2. Building performance characteristics prior to thermal retrofit

The study analysed a detached single-family house without a basement, built in 2002 in Szczecin (Climate Zone I, with a design outdoor temperature of $\theta_e = -16$°C [16]). The building has a large-scale form, without a habitable attic and includes an integrated garage.

Figure 1 presents the ground floor plan, including the layout and areas of the rooms as well as the design temperatures. The non-usable attic extends over the entire ground floor. The clear height of the ground floor is 2.6 m, and the maximum height of the attic is also 2.6 m. The knee wall height in the attic is 80 cm. Figure 2 shows an external view of the building.

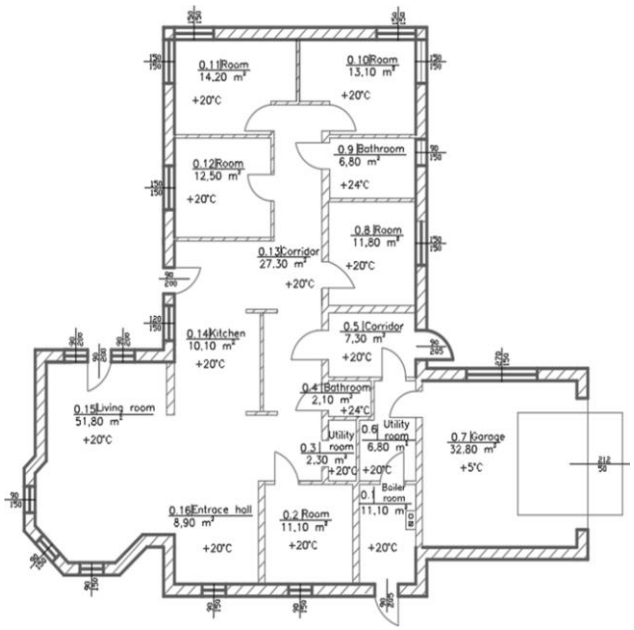

Fig. 1. Ground floor plan showing the layout and areas of the rooms, as well as the design temperatures for the analysed building.

Fig. 2. View of the analysed building.

The usable floor area is 225.80 m², and the building volume is 643.42 m³. The main entrance and garage are located on the western side. The ground floor comprises 16 rooms, including a boiler room with a separate external entrance. Due to the lack of thermal insulation in the external building partitions, heating costs were very high, prompting the decision to implement substantial thermal and energy upgrades. The attic was unheated and uninhabitable. The building's airtightness was assumed to

be $n_{50} = 6.0\ h^{-1}$. Ventilation was provided by gravity systems using existing masonry exhaust chimneys.

Prior to retrofit, the roof was covered with ceramic tiles and insulated with loosely laid mineral wool in the attic floor, with a thickness of 0.15 m. The external walls of the building were constructed from lightweight expanded clay concrete blocks with a thickness of 0.39 m, without internal insulation, and finished with gypsum board and plaster. Internal walls were made of hollow bricks measuring 120 mm × 250 mm × 63 mm, also without insulation. The intermediate floor slab between the ground floor and the unheated attic was made of reinforced concrete with a thickness of 0.10 m, covered with cement-bonded particle board, without insulation. The slab-on-grade ground floor structure consisted of sand, a concrete foundation layer, followed by 0.10 m of expanded polystyrene insulation, and finished with a floor compound and plywood. The windows were double-glazed, tilt-type, with polyvinyl chloride (PVC) frames, including balcony windows and two pairs of balcony doors.

The overall heat transfer coefficients for the building partitions were calculated using the Audytor OZC 7.0 Edu Pol software [17]. By comparing the calculated *U*-values with the maximum allowable values (U_{cmax}) specified in the Journal of Laws 2022 [18] on the technical conditions to be met by buildings and their location, it was observed that the roof, the intermediate floor slab below the unheated attic and the external wall did not meet current regulatory requirements due to the lack of insulation. Specifically, the roof's *U*-value exceeded the limit by 1.182 W/(m²·K), the ceiling by 0.426 W/(m²·K), and the external wall by 0.253 W/(m²·K). The total heat load prior to retrofit was 25 710 W, with 14 817 W attributed to the ground floor storey and 10 893 W to the non-habitable attic.

In its original state, the building did not meet the requirements in force at that time due to the absence of insulation in the external walls, roof and ceiling. This is confirmed by the thermal transmittance (*U*-value) prior to thermal retrofit, which was the main rationale for undertaking modernisation measures. The significant reduction in heat demand resulted from the poor initial condition of the building, not due to structural defects, but rather the lack of insulation in key partitions, which was the primary factor leading to very high heat losses.

2.1. Heat source and central heating system prior to modernisation

The boiler room has the following dimensions: a floor area of 6.90 m² and a volume of 17.53 m³. It featured both internal and external doors opening outward. Ventilation was provided via a 14 cm × 14 cm exhaust grille installed in the chimney shaft and a 14 cm × 14 cm supply grille mounted in the external wall, positioned 30 cm above the floor level.

The heat sources included a solid fuel boiler (wood-fired) and a liquefied gas boiler supplied from an underground propane tank located on the property. Switching between heat sources for the central heating system was performed manually by opening and closing the appropriate shut-off valves in the boiler room. During the autumn-winter heating season, the house was heated using a wood-fired boiler operating on the principle of generator gasification. The boiler was equipped with an exhaust fan to facilitate combustion. It had a nominal power output of 40 kW, a water capacity of 80 litres, and a fuel hopper capacity of 140 dm³. The seasonal wood consumption was approximately 40 m³. The system was designed to maintain a minimum return water temperature of 65°C, and the boiler efficiency ranged from 81% to 90% (according to the manufacturer technical specification). The boiler was connected via a flue outlet to a 150 × 150 mm steel chimney duct, which was routed through a shaft and extended above the roof.

In the spring-summer period, the house was heated using a liquefied gas boiler due to its lower fuel consumption for the domestic hot water system and occasional heating. The gas boiler was a single-function, wall-mounted unit with a power range of 8.9–21 kW and a closed type combustion chamber. It featured built-in weather-compensated control. The air/flue gas duct was made of steel with a diameter of 60/100 mm. The propane gas was supplied from an underground tank located on the property. A technical scheme of the heat source configuration prior to modernisation is presented in Fig. 3.

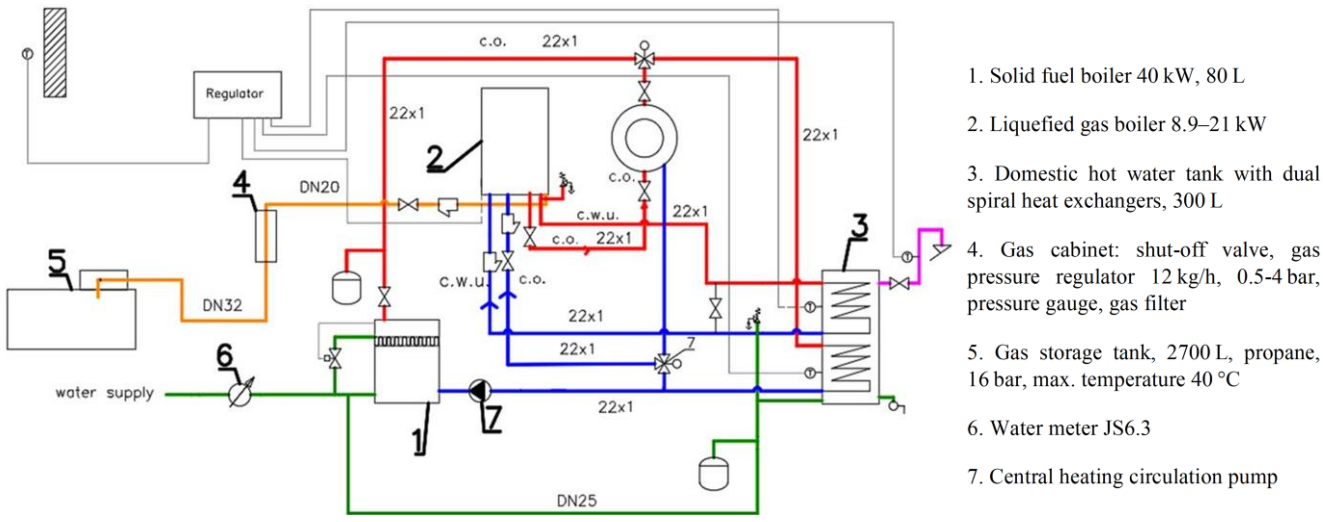

Fig. 3. Technical scheme of the heat source prior to retrofit.

The design temperatures of the heating water in the central heating system are 75°C/65°C. The system is a two-pipe installation embedded in the floor, with bottom connections made of copper pipes. Panel radiators type 22, featuring profiled heating plates and convective elements, equipped with thermostatic control valve inserts, were installed in the rooms. In the bathrooms, vertical pipe type radiators, made of non-alloy low-carbon steel, were used for heating.

During construction of the building, the dimensions of the radiators were selected and installed in such a way that their heating capacities were insufficient from the beginning to meet the high thermal loads of the rooms. As a result, it was difficult to maintain the design indoor temperature throughout the building. Additionally, the non-heated attic, lack of thermal insulation of the external walls, and the intermediate floor slab between the ground floor and attic contributed to significant heat losses from the heated spaces to the surroundings. The rooms cooled down rapidly, and users reported thermal discomfort as well as a noticeable increase in air humidity.

3. Building envelope components, thermal bridges, heat load

To ensure thermal comfort in the heated rooms, it is necessary to determine the heat flux that must be supplied to the space in order to compensate for all heat losses. The heat load calculations for the building's rooms were carried out in accordance with the PN-EN 12831:2006 Polish Standard [16], using the Audytor OZC 7.0 Edu Pol software [17]. The determination of the design heat load required to maintain the specified indoor design temperature under standardised design conditions, for the purpose of selecting an appropriate heat source, was performed as follows [14]:

$$\Phi_{HL} = \sum \Phi_{T,i} + \sum \Phi_{V,i} + \sum \Phi_{RH,i}, \tag{1}$$

where: $\Phi_{T,i}$ – transmission heat losses [W], $\Phi_{V,i}$ – ventilation heat losses [W], $\Phi_{RH,i}$ – additional heating power required to compensate for reduced heating performance (reheat) [W].

In the calculation of the design heat loss due to transmission, the following components are considered: direct heat losses to the external environment, heat losses through unheated spaces to the outside, heat losses to the ground, and heat transfer between heated zones with different indoor temperatures [16]:

$$\Phi_{T,i} = [\sum_k (A_k U_k e_k) + \sum_l (\psi_l l_l e_l) + \sum_k (A_k U_k b_u) + \\ + \sum_l (\psi_l l_l b_u) + f_{g1} f_{g2} \sum_k (A_k U_{equiv,k}) G_w + \\ + \sum_k f_{ij} A_k U_k] \left(\theta_{int,i} - \theta_e\right), \tag{2}$$

where: A_k – area of building element (k) [m^2], U_k – heat transfer coefficient of the building envelope components (k) [W/(m^2·K)], e_l, e_k – correction factors for orientation, taking into account climatic influences, ψ_l – linear thermal transmittance coefficient (l) [W/(m·K)], l_l – length (l) of the linear thermal bridge between the internal and external environments [m], b_u – temperature reduction coefficient accounting for the difference between the temperature of the unheated space and the design external temperature [-], f_{g1} – correction factor accounting for the influence of annual fluctuations in outdoor temperature, f_{g2} – temperature reduction factor accounting for the difference between the annual average outdoor temperature and the design outdoor temperature, $U_{equiv,k}$ – equivalent heat transfer coefficient of a building element (k) [W/(m^2·K)], G_w – correction factor for groundwater influence, f_{ij} – temperature reduction factor accounting for the difference between the temperature of the adjacent space and the design outdoor temperature, $\theta_{int,i}$ – design indoor temperature of the heated space (i) [°C], θ_e – design outdoor temperature [°C].

The ventilation heat loss is determined using the following equation [16]:

$$\Phi_{V,i} = \dot{V}_l \rho c_p \left(\theta_{int,i} - \theta_e\right), \tag{3}$$

where: $\dot{V}_i$ – volumetric flow rate of ventilation air supplied to the heated space [m^3/s].

The reheat amount includes the correction factor f_{RH}, which depends on the heating-up time and the assumed indoor temperature setback during reduced heating periods [16]:

$$\Phi_{RH,i} = A_i f_{RH}, \tag{4}$$

where: A_i – area of the heated space [m^2], f_{RH} – correction factor accounting for heating-up dynamics and temperature setback [W/m^2]. In the presented analysis, this component of the building's thermal load balance was not considered, as the occupants do not utilise this function. According to standard [16], the reheat amount is not mandatory.

As part of the preparation for the building's thermal retrofit, the initial step involved an analysis of heat losses through linear thermal bridges. The assessment of temperature distribution within thermal bridge models, along with the determination of heat flux passing through these elements, enabled the proposal of design solutions aimed at reducing linear heat losses. Surface thermal bridges, such as glazed area and door leaf surface area, were incorporated into the heating load calculations using the software referenced in [17]. Point thermal bridges were not included in the analysis.

The lengths of thermal bridges in the presented analysis were modelled using Therm Software 7.8.77, which is based on the PN-EN ISO 10211-2 standard [19]. According to this standard, the geometric model of a thermal bridge must be created under strictly defined thermal and geometric boundary conditions. The lengths of thermal bridges are assumed to be three times the total thickness of the adjoining partitions or at least 1 m from the central element.

Table 1 presents the models of linear thermal bridges in the building, developed in accordance with the PN-EN ISO 10211:2008P standard [19], using Therm Software version 7.8.77 [20]. The first column provides a visual representation and designation of each thermal bridge type. The second and third columns illustrate the temperature distribution models for each thermal bridge in two scenarios: prior to and after the building retrofit.

Table 1 is supplemented with a colour scale legend and boundary temperature data for the building envelope components.

Table 1. Temperature distribution in building thermal bridges – models generated using Therm Software 7.8.77 [20].

Thermal bridge	Temperature distribution in building thermal bridges	
	Prior to thermal retrofit	After thermal retrofit
	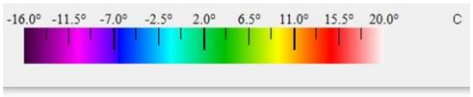	
 External corner (a)	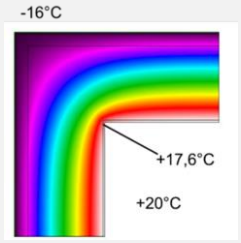	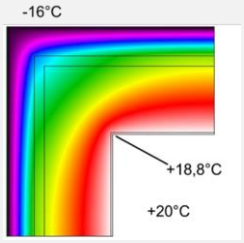
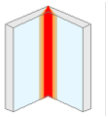 Internal corner (b)	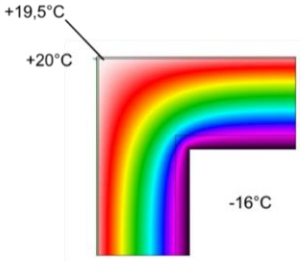	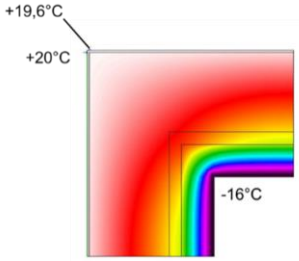
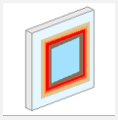 Exterior wall section adjacent to fenestration opening (c)	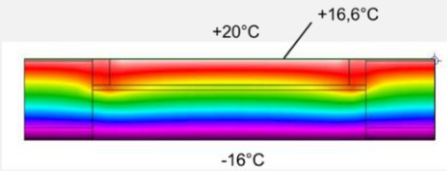	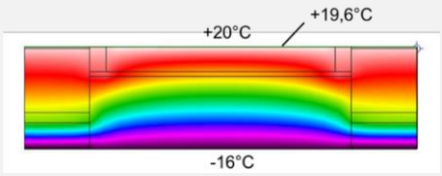
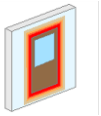 Exterior wall section adjacent to door opening (d)	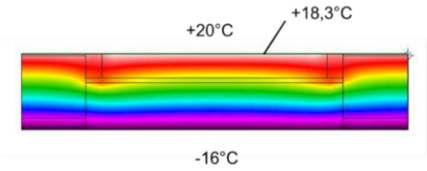	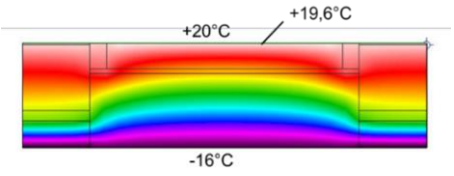
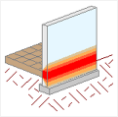 Slab-on-grade floor system / exterior wall interface (e)	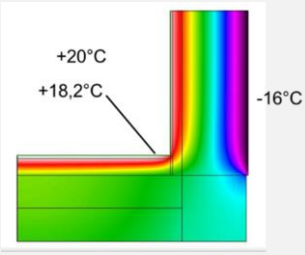	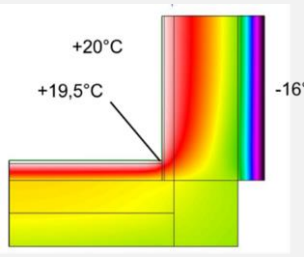
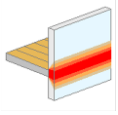 Intermediate floor structure / exterior wall junction (f)	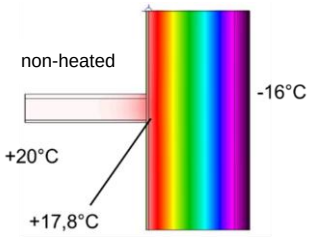	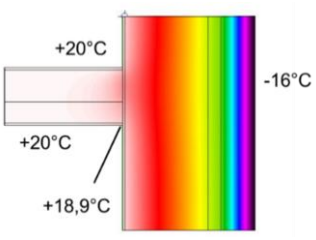

For the external corner (convex corner) thermal bridge (a), the analysis of temperature distribution within the building envelope component prior to and after insulation revealed a significant improvement in thermal performance following the retrofit. Prior to insulation, low-temperature isotherms penetrated deeply into the structure, indicating substantial heat losses and a heightened risk of water vapour condensation. After the application of thermal insulation, a distinct outward shift of the isotherm lines was observed, demonstrating the effectiveness of the implemented insulation strategy. The total heat transfer coefficient (*U*-value) for this thermal bridge, under a temperature gradient of 36 K (−16°C exterior and +20°C interior), was reduced from 0.556 W/(m²·K) to 0.111 W/(m²·K).

The analysis of the internal corner (concave corner) thermal bridge (b) revealed similar phenomena, albeit with greater intensity. Prior to insulation, the temperature on the interior surface of the envelope at the corner was significantly lower than in other areas of the partition, indicating intense heat transfer and a high risk of water vapour condensation. Following the application of thermal insulation, the isotherms shifted toward the outer edge of the envelope, and the local temperature minimum increased. The total heat transfer coefficient (*U*-value) for this thermal bridge decreased from 0.537 W/(m²·K) to 0.141 W/(m²·K).

The next component of the analysis was the exterior wall section adjacent to the fenestration opening (c). Before the detail was improved, significant cooling of the envelope was observed in the area where the window frame connects to the masonry wall. Temperatures near the window reveal dropped locally to critical levels. After implementing an improved installation method and adding thermal insulation in the reveal zone, the low-temperature isotherms shifted toward the outer part of the envelope. The temperature at critical points increased significantly, indicating effective elimination of the local linear thermal bridge and improved energy performance of the entire construction detail. The *U*-value was reduced from 0.241 W/(m²·K) to 0.095 W/(m²·K).

In the analysis of the exterior wall section adjacent to door opening, and thermal bridge occurring between the door assembly and the external wall (d), the initial condition revealed significant thermal anomalies. The zone surrounding the door, particularly near the ground level, exhibited pronounced cooling and intense heat flux, contributing to localised energy losses and a reduction in thermal comfort. Following the implementation of additional thermal insulation, these adverse phenomena were substantially mitigated. The isotherms in this region became more uniform, and the temperature values within the building envelope increased, indicating improved thermal conditions and reduced potential for energy loss. The total modelled *U*-value decreased from 0.208 W/(m²·K) to 0.096 W/(m²·K).

The next analysed thermal bridge, slab-on-grade floor system/exterior wall interface, was located at the junction between the internal wall and the ground-bearing floor slab (e). This area is particularly susceptible to thermal bridging due to its direct contact with the subsoil, which typically maintains a significantly lower temperature.

In the pre-retrofit condition, the simulation revealed a distinct temperature drop in the internal corner, posing a risk of surface condensation. After applying additional insulation in the plinth zone, the low-temperature isotherms shifted deeper into the external envelope, and the temperature within the corner increased to a level ensuring both thermal and hygienic safety. The overall heat transfer coefficient was reduced from 0.336 W/(m²·K) to 0.162 W/(m²·K).

The final case analysed involved a thermal bridge at the junction between the exterior wall and the intermediate floor slab separating the building storeys (f). In the initial scenario – prior to thermal retrofitting, when the attic was uninsulated and unheated, the simulation clearly indicated heat losses through the uninsulated portion of the floor slab, which structurally penetrated the thermal insulation layer of the external wall. This area exhibited significant cooling, with the minimum local temperature dropping to a level conducive to water vapour condensation. After the application of additional insulation in the floor slab region, the isotherms became smoother and shifted, indicating a substantial improvement in thermal conditions. The thermally upgraded building envelope ensured continuity of the insulation layer, thereby minimising energy losses and enhancing the durability of the building structure. In the thermal simulation, the total *U*-value coefficient for this thermal bridge, under a temperature gradient of 36 K, was reduced from 0.225 W/(m²·K) to 0.165 W/(m²·K).

4. Building performance characteristics after thermal retrofit. Result analysis.

A thermal retrofit project was developed for the building, based on the following interventions:

- insulation of external walls using expanded polystyrene (EPS) with a thermal conductivity of k = 0.040 W/(m·K) and a thickness of 0.15 m,
- roof insulation with mineral wool k = 0.052 W/(m·K), applied in a layer of 0.35 m thickness,
- replacement of the roof covering from ceramic tiles to metal roofing sheets k = 50 W/(m·K), aimed at reducing the structural load on the roof,
- insulation of the intermediate floor slab between the ground floor and the attic using EPS k = 0.040 W/(m·K) with a thickness of 0.15 m,
- sealing of window and door frames to improve airtightness and reduce uncontrolled infiltration.

Based on literature data indicating the limited impact of window and door replacement on the overall heat demand reduction estimated at approximately 3% according to [6] and considering the high investment costs associated with such measures, the investors opted not to include fenestration replacement in the scope of thermal retrofit. Additionally, a design was developed to convert the attic into a habitable and heated space, including the layout of new rooms and the integration of a heating system. New stairs were also planned to enable users to move between floors, replacing the previously existing ladder that provided access only to the non-usable attic. To enhance thermal comfort

on the external façade, the installation of electrically operated external window shutters, integrated into the window frames, was proposed as part of the building insulation works. In the case of the garage, it was designated to be heated to an indoor temperature of t_i = +5°C. Consequently, the internal garage walls were insulated in accordance with the envelope specifications outlined in [18]. The building occupants chose to retain natural (gravity-based) ventilation. Airtightness of the building envelope was improved to the design level of n_{50} = 2.0 h^{-1}, achieved through sealing of window and door frames, insulation of external partitions and sealing of service penetrations. For retrofitted buildings without mechanical ventilation, the typical airtightness level after modernisation falls within the range of n_{50} = 2.0–3.5 h^{-1} [6]. In the analysed case, a value of n_{50} = 2.0 h^{-1} was adopted, reflecting the effect of careful insulation of building partitions, improved continuity of insulation at structural joints, and the proposed use of external roller shutters by occupants. According to available data on airtightness measurements for retrofitted buildings, such measures can enable achieving n_{50} values below 3.0 h^{-1}.

For the proposed thermal retrofit measures, calculations of the overall heat transfer coefficients were performed using the Audytor OZC 7.0 software Edu Pol [17] in accordance with the standard [16]. The results are presented in Table 2. Due to the modernisation of the building's heat source, the total heating load of the building was also calculated and summarised in Table 3. All calculations were carried out for both analysed scenarios, prior to and after thermal retrofit.

Table 2. Values of the overall heat transfer coefficient (*U*-value) for the building partitions, calculated using Audytor OZC 7.0. Edu Pol [17].

Building Partition type	Area of partitions [m²]	Overall heat transfer coefficient *U* [W/(m²·K)]		
		Prior to thermal retrofit	After thermal retrofit	$U_{c(max)}$ [18] [W/(m²·K)]
Roof	269.01	1.332	0.143 (reduction by 89,3%)	0.150 ($t_i \geq 16°C$)
External door	33.75	1.300	1.300	1,300
External window	41.40	0.900	0.900	0.900 ($t_i \geq 16°C$)
Intermediate floor slab	218.73	0.576	0.180 (reduction by 68.8%)	1.000 ($\Delta t_i \geq 8°C$)
Slab-on-grade floor	224.96	0.200	0.196 (reduction by 2%)	0.300 ($t_i \geq 16°C$)
Internal wall	412.04	0.968	0.911 (reduction by 5.9%)	1.000 ($\Delta t_i \geq 8°C$)
External wall	696.51	0.453	0.168 (reduction by 63.3%)	0.200 ($t_i \geq 16°C$)

Table 3. Heat loads for rooms and the building, and the design indoor temperatures, calculated using Audytor OZC 7.0 Edu Pol [16,17].

Type of room	Temperature $\theta_{int,i}$ [°C]		Heat load Φ_{HL} [W]	
	Prior to thermal retrofit	After thermal retrofit	Prior to thermal retrofit	After thermal retrofit
Ground floor				
Boiler room	20	20	871	333
Room	20	20	703	338
Utility room without window	20	20	18	9
Bathroom without window	24	24	200	112
Corridor	20	20	446	233
Utility room without window	20	20	403	232
Garage	non-heated	5	2320	825
Room	20	20	632	274
Bathroom	24	24	701	377
Room	20	20	1247	452
Room	20	20	1377	557
Room	20	20	716	345
Corridor	20	20	448	396
Kitchen	20	20	837	410
Living room	20	20	3051	1317
Entrance hall	20	20	847	289
Attic (residential)				
Room	non-heated	20	10893	845
Bathroom without window	non-heated	24		621
Corridor	non-heated	20		381
Room	non-heated	20		1130
Sum			25710 (25.7 kW)	9476 (9.5 kW)

A heat load value is obtained for the unheated attic because heat transfer from the heated zones to adjacent unheated spaces must be considered in accordance with standard calculation procedures (EN 12831 [16]). The attic, although not heated, receives heat through the ceiling and thermal bridges, and its temperature is typically lower than that of the conditioned space. This results in a heat flow that contributes to the overall heating demand of the building.

The proposed thermal retrofit measures resulted in the following changes in the calculated thermal transmittance (*U*-values) for individual building components:

- roof: U = 0.143 W/(m^2·K), representing a reduction of 1.189 W/(m^2·K) due to the implemented improvements,
- intermediate floor slab (between ground floor and the non-heated attic): U = 0.180 W/(m^2·K), corresponding to a decrease of 0.396 W/(m^2·K),
- slab-on-grade floor: U = 0.196 W/(m^2·K), with a marginal reduction of 0.004 W/(m^2·K).

The total design heat loss for the thermally modernised building, based on characteristic parameters from Journal of Laws 2022 [18], amounted to 9476 W, indicating a reduction of 16 234 W. This includes a decrease for the ground floor storey from 14 817 W to 5814 W, and on the attic level from 10 893 W to 3662 W (from the uninhabitable attic to the residential attic).

To improve the quality conclusions and enable a comprehensive assessment of the thermal retrofit, two tables (Table 4 and Table 5) presenting the components of the building's heat load have been added. Additional demand from converting an unused attic into living spaces is presented in Table 3. In the presented analysis, the reheat component of the building's thermal load balance was not considered, as the occupants do not utilise this function. According to standard [16], the reheat amount is not mandatory. Since the gas boiler is a single-function unit operating in conjunction with a domestic hot water heater, and the number of occupants (four persons) as well as the presence of two bathrooms remain unchanged before and after thermal retrofitting, the domestic hot water demand also remains constant at 20 kW, assuming a high level of domestic hot water thermal comfort.

Tables 4 and 5 present the distribution of individual components to the building's heat balance before and after thermal retrofitting. Heat transmission losses were divided into two categories:

(1) losses through external envelope components, calculated as the sum of products $A_k \cdot U_k \cdot e_k$,

(2) losses through partitions adjacent to unheated spaces (e.g. attic or garage), in accordance with the methodology of PN-EN 12831 [16].

Additionally, (3) linear losses caused by thermal bridges were considered separately, calculated using the relation $\psi_l \cdot l_l \cdot e_l$. Losses due to minimum ventilation (V_{min}) are lower than infiltration ventilation losses (V_{inf}) and, therefore, were not included in accordance with standard [16]. After thermal retrofitting, losses associated with unheated spaces were eliminated, as all rooms are heated following the modernisation.

Table 4. Distribution of heat load components in the building prior to thermal retrofit.

Type of room	Heat losses by transmission - external partitions [W]	Heat losses by transmission to unheated spaces [W]	Linear heat losses - thermal bridges [W]	Ventilation heat losses - infiltration [W]	Total heating load [W]
Boiler room	643	120	31	77	871
Room	354	152	24	173	703
Utility room without window	0	6	0	9	18
Bathroom without window	0	33	0	167	200
Corridor	202	100	31	113	446
Utility room without window	0	297	0	106	403
Garage	1813	0	77	430	2320
Room	268	159	22	183	632
Bathroom	456	109	19	117	701
Room	820	179	44	204	1247
Room	923	188	45	221	1377
Room	334	156	32	194	716
Corridor	0	224	0	224	448
Kitchen	359	249	72	157	837
Living room	1675	402	169	805	3051
Extrance hall	445	247	17	138	847
Attic (non-heated)	6666	0	2069	2160	10893
Total	14958	2621	2652	5478	25710

Table 5. Distribution of heat load components in the building after thermal retrofit.

Type of room	Heat losses by transmission - external partitions [W]	Heat losses by transmission to unheated spaces [W]	Linear heat losses-thermal bridges [W]	Ventilation heat losses - infiltration [W]	Total heating load [W]
Boiler room	238	0	31	64	333
Room	141	0	24	173	338
Utility room without window	0	0	0	9	9
Bathroom without window	76	0	0	36	112
Corridor	89	0	31	113	233
Utility room without window	126	0	0	106	232
Garage	169	0	59	597	825
Room	69	0	22	183	274
Bathroom	241	0	19	117	377
Room	204	0	44	204	452
Room	292	0	44	221	557
Room	119	0	32	194	345
Corridor	72	0	0	324	396
Kitchen	203	0	50	157	410
Living room	368	0	144	805	1317
Extrance hall	134	0	17	138	289
Attic (residential)					
Room	199	0	169	481	845
Bathroom without window	169	0	128	324	621
Corridor	180	0	53	148	381
Room	215	0	8	807	1130
Total	3304	0	875	5201	9476

The tables provide a detailed breakdown of heat loss components for individual rooms in the building before and after thermal retrofitting. Comparing these data allows identification of the elements of the heat balance that contributed most to the achieved energy savings. (1) Insulation of external partitions. The greatest impact on reducing the heat load resulted from the decrease in transmission losses through external envelope components, which dropped from 14 958 W to 3304 W, representing a 78% reduction. (2) Elimination of losses to unheated spaces. Prior to modernisation, a significant portion of losses originated from heat transfer from the ground floor to the unheated attic (2621 W). After retrofitting, the attic became a heated space, eliminating these losses entirely. (3) Reduction of thermal bridges, insulating structural details and improving window reveals and wall junctions reduced linear losses from 2652 W to 875 W, a 67% decrease, highlighting the substantial role of thermal bridges in the overall heat balance. (4) Ventilation losses decreased from 5478 W to 5201 W (a 5% reduction), primarily due to improved airtightness and reduced uncontrolled infiltration. Collectively, these measures resulted in a 63% reduction in the building's total heat load.

4.1. Heat source and central heating system after modernisation

The location of the boiler room remains unchanged. The solid fuel central heating boiler, along with all associated equipment, has been removed from the room. The chimney previously used for flue gas discharge remains in place but will no longer be in use. The gas-fired boiler continues to operate in its original location without modification. The burner of this boiler can operate not only on liquefied petroleum gas, but also, after appropriate adjustment, on natural gas. Additionally, the heat source has been supplemented with flat-plate solar collectors and associated equipment, which have been connected to the existing bivalent domestic hot water heater. For the purpose of automatic regulation of the modernised heat source, a new controller has been installed in the boiler room. Furthermore, the central heating circulation pump has been replaced with a modern single-speed circulating pump.

The burner of the existing gas boiler has been adapted for operation with network-distributed natural gas GZ50; however, its factory settings will be adjusted due to the change in the type of fuel used (modified power output range 11–23 kW). The fuel will be delivered to the boiler from the existing gas distribution network via a gas connection routed across the property. The underground liquefied gas tank has been decommissioned, as it became feasible to design a direct gas connection to the network, thereby reducing the inconvenience associated with fuel delivery and tank maintenance. The tank had been in use for approximately 20 years, which would soon necessitate its replacement, incurring additional costs. A gas connection has been installed from the gas network to a cabinet mounted on the building wall. The distance between the gas cabinet and the street is 12 meters. A 1.5-meter section of the connection from the cabinet was constructed using steel piping, while the remaining section was

made of PE pipe. The pipes were laid 0.6 meters below the ground level with a slope of 4‰. Inside the gas cabinet mounted on the building, a self-actuating pressure regulator with two-stage pressure reduction has been installed. The regulator includes an integrated shut-off valve, an overpressure quick-closing valve at the inlet, and a mesh filter. Additionally, a gas meter with a maximum flow rate of 4 m^3/h and a stainless steel shut-off valve have been installed.

To support the domestic hot water (DHW) system, flat-plate solar collectors with a total surface area of 3×2.06 m² were selected. The selected collector area covers 100% of the average daily DHW demand of the building's occupants during the summer period. The collectors were installed on the roof, facing southwest, due to optimal solar exposure on that side of the building (see Fig. 4). The building is located in Szczecin, at a latitude of 53°23'N, where the average annual total sunshine duration is approximately 1700–1800 hours/year, and the annual average solar radiation on a horizontal surface amounts to 1000−1100 kWh/m²/year [21].

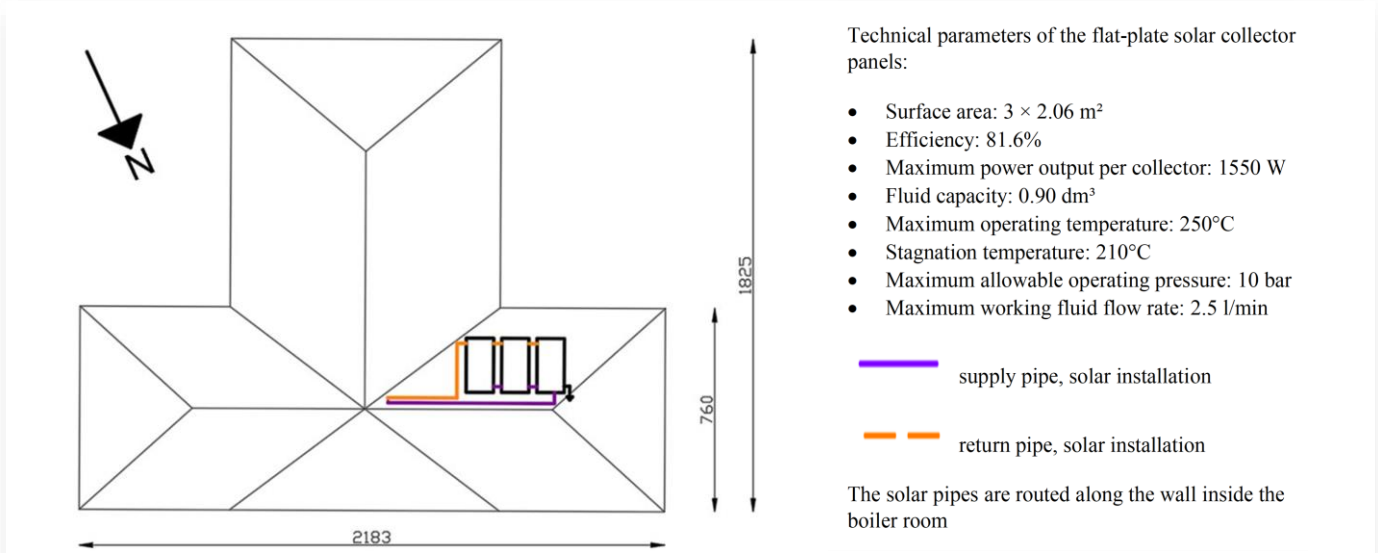

Fig. 4. Arrangement of flat-plate solar collectors on the building roof.

The existing dual-coil domestic hot water (DHW) heater with a capacity of 300 dm³, previously used in conjunction with a solid fuel boiler, has been retained and integrated with the flat-plate solar collector system. Overheating protection for the DHW system has been designed and is illustrated in the heat source schematic (see Fig. 5).

Cold water is routed and connected to the DHW line via a three-way valve, allowing cold water to be introduced into the system when the DHW temperature exceeds the maximum permissible level, thereby cooling the medium. The solar installation is protected by a safety valve and a closed expansion vessel with a volume of 18 litres. Additionally, a vent has been installed on the roof to facilitate air removal from the system during fluid replacement or refilling.

The design temperatures of the heating system water are 55°C / 45°C. Due to insufficient thermal output of the existing radiators and piping, a complete replacement of all heaters and distribution lines was designed. The new hydronic heating system utilises modern plastic piping technology, consisting of multilayer polyethylene pipes with an aluminium diffusion barrier. The distribution network is routed through individual rooms within the thermal insulation layer of the structural floor

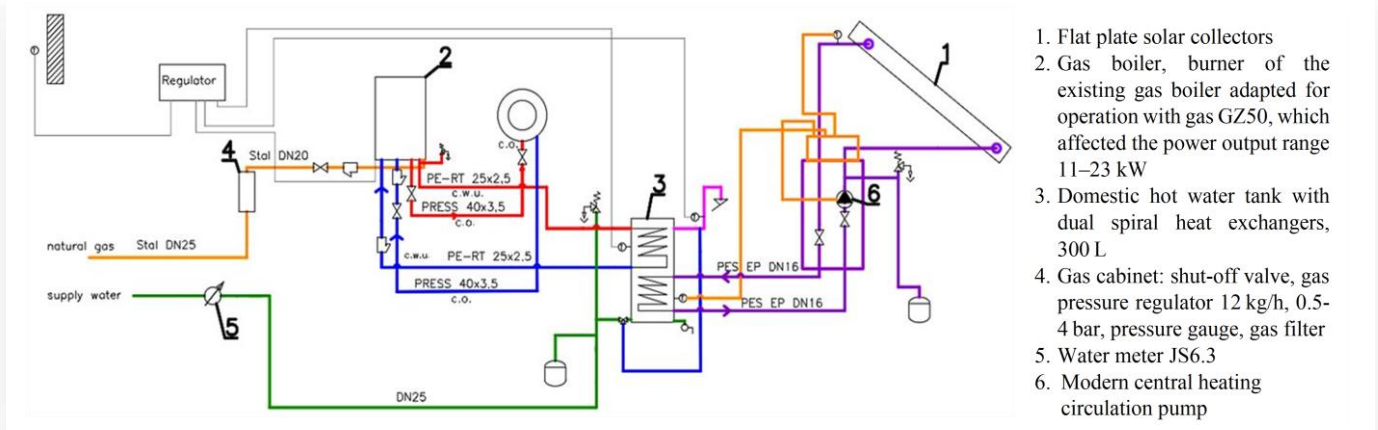

Fig. 5. Technical scheme of the heat source after modernisation.

slab and connected to the designated radiators using a tee-branch configuration. Panel radiators were specified for general spaces. For the bathroom zone, modern bathroom type radiators were selected, characterised by flat heating surfaces, providing both functional and aesthetic integration with the interior.

5. Conclusions

The integrated thermal retrofit project for the single-family building located in Szczecin was undertaken due to the absence of thermal insulation in the external walls and roof structure. This deficiency resulted in high operating costs for the users, caused by excessive heat losses, rapid cooling of the building, and the inconvenience of restoring indoor thermal comfort during the winter season. The lack of building envelope insulation led to increased energy demand for space heating in winter and reduced passive protection against overheating in summer, thereby compromising thermal comfort and energy efficiency.

Calculations and analysis of the overall heat transfer coefficient (*U*-values) of the building envelope components in their existing condition, including thermal bridges and heat source performance, enabled the formulation of targeted thermal and technical modernisation measures. The comparative assessment of the building's thermal performance before and after retrofitting demonstrated that comprehensive thermal retrofit would significantly reduce the total heating load, from 25 710 W to 9476 W. This reduction of over 63% provided a reduction in the useful heat output of the heat source and a shorter operating time, which is relevant in the context of using fossil fuels, for example natural gas. The substantial decrease in thermal demand highlights the high energy-saving potential resulting from the following interventions: thermal insulation of external walls, insulation of the intermediate floor slab, roof insulation, and replacement of the roof covering.

Based on the analysis of temperature distribution in building thermal bridge models conducted using the Therm 7.8.77 software [18], it was determined that existing linear thermal bridges contribute significantly to the overall heat losses, with the corresponding thermal heat transfer values being relatively high. Thermal retrofitting measures, including additional insulation and airtightness improvements at thermal bridge locations, were proposed. The simulation results indicated that, for selected construction details, the application of supplementary insulation led to a reduction in the *U*-value by more than 50%. This highlights the necessity of accounting for thermal bridges in energy retrofit projects, not only from the perspective of energy efficiency but also in terms of thermal comfort, hygienic conditions, and the durability of building envelopes. The computational results and temperature distribution visualisations confirm that thermal retrofitting effectively eliminates local zones of reduced surface temperature in the analysed thermal bridge areas, thereby reducing the risk of surface condensation and mould growth in practice.

The modernisation of the building's existing heat source, involving the replacement of an outdated solid fuel boiler system with a new central heating installation powered by a natural gas-fired condensing boiler, along with the proposed integration of flat-plate solar collectors for domestic hot water (DHW) support, contributed to a reduction in CO_2 emissions and decreased dependence on solid fuels and local fuel storage systems.

As a result of the design solutions prepared for the building owner, the boiler room was upgraded, flat-plate solar collectors were installed on the roof, and the DHW system was modernised. Furthermore, a decision was made to prepare an application for external state funding to support the thermal retrofitting of the building envelope in the near future. Further research, including thermographic inspections and in-situ measurements of the actual *U*-values of the building envelope components, is planned to be conducted prior to, during and after the implementation of the envelope modernisation works.

The findings presented in this study can be extrapolated to a broader category of buildings located within Polish Climate Zone I and regions exhibiting comparable thermal load characteristics. The case study building represents a typical structural configuration of single-family houses constructed in the early 2000s, characterised by uninsulated external walls made of lightweight aggregate concrete blocks, a reinforced concrete floor slab without thermal insulation, and insufficient roof insulation. The observed 63% reduction in heating load, achieved through thermal insulation of building envelopes and mitigation of linear thermal bridges, may serve as a reference benchmark for buildings with similar geometric, material and operational parameters. The post-retrofit overall heat transfer coefficients (*U*-values) comply with the requirements specified in [18] for residential buildings, indicating that the adopted insulation strategy can be considered a model configuration for structures located in Climate Zone I. Furthermore, the analysis of thermal bridges confirms that, under temperature differentials of approximately 36 K, reductions in linear thermal transmittance of up to 50% are attainable. This finding is particularly relevant for buildings situated in northern regions of the country, where the influence of thermal bridges on energy losses is amplified by the extended heating season.

Acknowledgements

The authors would like to express their sincere gratitude to Ms Jadwiga Wawer-Bernat, the owner of the analysed building, for her kind cooperation and for granting access to the property for the measurements necessary to conduct this research. Her trust and support were significant to the successful completion of this study.

This article is a revised and expanded version of a paper entitled: Impact of thermal modernisation including heat source upgrade on heat load of an existing single-family building (in Polish), which was presented at the 17th Heat and Mass Transfer Symposium, Kielce, Poland, September 8−10, 2025 [22].

References

[1] *Thermal modernization of a building – what is it and what does it include*). *Izolacje*. https://www.izolacje.com.pl/artykul/sciany-stropy/186640,termomodernizacja-budynku-co-to-jest-i-co-obejmuje-1 [Accessed 20 Jun. 2025] (in Polish).

[2] Dz. U. 2024, item 1446. *Act of 21 November 2008 on Supporting Thermal Modernization and Renovations and on the Central Register of Building Emissions* (consolidated text). Journal of Laws of the Republic of Poland, 2024 (in Polish).

[3] Pawłowski, K. (2020). Thermal modernization of buildings considering heat and moisture requirements from January 1, 2021. *Izolacje*, 2, 19–31 (in Polish).

[4] Krause, P. (2010). Energy effects of thermal modernization of a residential building. *Fizyka Budowli w Teorii i Praktyce*, 5(2), 45–49 (in Polish).

[5] Zawada, B., & Rucińska, J. (2021). Optimization of modernization of a single-family building in Poland including thermal comfort. *Energies*. 14(10), 2925. https://doi.org/10.3390/en14102925

[6] Oleniacz, R, Kosietczak, M, & Rzerzutek, M. (2014). Assessment of thermal modernization effects in single-family buildings. 1. Reduction of heat consumption and pollutant emissions to air. *Czasopismo Inżynierii Lądowej, Środowiska i Architektury*, 23(61/3/I),183–196. doi: 10.7862/rb.2014.55 (in Polish).

[7] Koczyk, H, & Antoniewicz, B. (2000). *Heating: fundamentals of thermal design and building thermal modernization*. Wydawnictwo Politechniki Poznańskiej, Poznań (in Polish).

[8] Kurtz, K, & Gawin, D. (2009). *Energy certification of residential buildings with examples*. Wrocławskie Wydawnictwo Naukowe Atla 2, Wrocław (in Polish).

[9] Mayer, Z, Kahn, J, Götz, M, Hou, Y., Beiersdörfer, T., Blumenröhr, N., Volk, R., Streit, A., & Schultmann, F. (2023). Thermal bridges on building rooftops. *Scientific Data*, 10(268), 1–8. doi: 10.1038/s41597-023-02140-z

[10] Pawłowski, K. (2018). Thermal modernization and thermal bridges in construction. *Przewodnik Projektanta*, 2, 0–14 (in Polish).

[11] Levinskytė, A., Banionis, K., & Geležiūnas, V. (2016). The influence of thermal bridges for buildings energy consumption of "A" energy efficiency class. *Journal of Sustainable Architecture and Civil Engineering*. 15(2), 47–58. doi: 10.5755/j01.sace.15.2.15351

[12] Żarski, K. (2008). Possibilities of meeting energy performance requirements of buildings in light of new legal regulations. *INSTAL*, 12, 6–11 (in Polish).

[13] Pawlak, F. (2016). Impact of thermal bridges on heat losses and energy performance of buildings. Methods of accounting for thermal bridges in calculations. *INSTAL*, 6, 24–29 (in Polish).

[14] Wiącek, A., Werle, S., & Ruszel, M. (2025). The impact of the behaviour of individual users in single-family households on the values of internal heat gains in a building. *Archives of Thermodynamics*, 46(2), 173–183. doi: 10.24425/ather.2025.154916

[15] Turoń, M.K. (2024). Operation of a hybrid heating system based on heat pumps using a photovoltaic installation. *Archives of Thermodynamics*, 45(4), 153−162. doi: 10.24425/ather.2024.152004

[16] PN-EN 12831:2006. *Heating systems in buildings – Method for calculating design heat load* (in Polish).

[17] *Audytor OZC 7.0. Pro Edu, Sankom*. https://pl.sankom.net/oprogramowanie/edukacyjne [Accessed 15 Mar. 2025].

[18] Dz. U. 2022, item 1225. *Ministry of Development and Technology. Announcement of 15 April 2022 on the publication of the consolidated text of the Regulation of the Minister of Infrastructure on the technical conditions to be met by buildings and their location*. Journal of Laws. 2022 (in Polish).

[19] PN-EN ISO 10211:2008P. *Thermal bridges in buildings – Heat flows and surface temperatures – Detailed calculations* (in Polish).

[20] *THERM Software 7.8.77. Berkeley Lab*. https://windows.lbl.gov/therm-software-downloads [Accessed 20 Mar. 2025].

[21] Masłowski, A. *Solar energy in Poland – insolation. Poradnik Projektanta*. https://poradnikprojektanta.pl/energia-sloneczna-w-polsce-naslonecznienie/ [Accessed 25 Mar. 2025] (in Polish).

[22] Bernat, W., Zwarycz-Makles, K. (2025). Impact of thermal modernization including heat source upgrade on heat load of an existing single-family building. *17th Heat and Mass Transfer Symposium*. 8–10 September, Kielce, Poland.